

# Direct Numerical Simulations of Fundamental Turbulent Flows with the Largest Grid Numbers in the World and its Application of Modeling for Engineering Turbulent Flows

Group Representative

Chuichi Arakawa Japan Atomic Energy Research Institute

Authors

Chuichi Arakawa Japan Atomic Energy Research Institute

Oliver Fleig The University of Tokyo

Takashi Ishihara Nagoya University

Yukio Kaneda Nagoya University

Databases of incompressible turbulence obtained by high-resolution direct numerical simulations (DNSs) with the number of grid points up to  $4096^3$  were systematically analyzed on the Earth Simulator (ES). The DNSs consist of two groups; one is with  $K_{\max}\eta = 1$  and the Taylor micro scale Reynolds number  $R_\lambda = 167\sim 1131$ , while the other is with  $K_{\max}\eta = 2$  and  $R_\lambda = 94\sim 675$ , where  $K_{\max}$  is the maximum wave number and  $\eta$  the Kolmogorov length scale. Reynolds number dependence of various turbulence statistics, which include higher-order moments of velocity derivatives, the energy spectra in the near-dissipation wavenumber range, pressure spectra, were investigated. Visualization of high intensity regions of vorticity, strain, and the gradient of pressure obtained by high-resolution DNS was also performed. An engineering application is also studied. The physical mechanisms associated with broadband tip vortex noise caused by rotating wind turbines are investigated. The flow and acoustic field around a wind turbine blade is simulated using compressible Large Eddy simulation and direct noise simulation, with emphasis on the blade tip region. The far field aerodynamic noise is modeled using acoustic analogy. Aerodynamic performance and acoustic emissions are predicted for the actual tip shape and an ogee type tip shape. For frequencies above 4 kHz a decrease in sound pressure level by 5 dB is observed for the ogee type tip shape. It is hoped that the simulation results will contribute towards designing new wind turbine blades for reduced noise emission.

**Keywords:** incompressible turbulence, high-resolution DNS, visualization, LES, Wind turbine, Noise reduction

## 1. Data analyses based on high-resolution DNSs of incompressible turbulence

In order to study universal nature of turbulence, we performed a series of direct numerical simulations (DNSs) of forced incompressible turbulence with the number of grid points up to  $4096^3$  on the Earth Simulator (ES). Each run (except for  $N = 4096$ ) was carried out until  $t = t_f$ . Since  $u'^2 = 2E/3$  and  $E = 0.5$  in our runs, one eddy turn over time  $T = L / u'$  is about 2, in each run, so that  $t_f \sim 5T$  except for  $N = 4096$ , where  $u'$  is the rms of one velocity component and  $L$  the integral length scale. In series 1 and 2, we set the values of kinematic viscosity  $\nu$  and the maximum wave number  $K_{\max}$  so that  $K_{\max}\eta \sim 1$  and 2, respectively. The maximum of the Taylor micro-scale Reynolds number  $R_\lambda$  was obtained for  $N = 4096$  in series 1. The maximum value ( $R_\lambda \sim 1130$ ) is much larger than the largest values ( $R_\lambda \sim 470$ ) before the appearance of the

ES, and the ratio of  $L$  to  $\eta$  in the turbulence at  $R_\lambda \sim 1130$  is over 2000. The set of DNS data has potential ability to elucidate the universal nature of the high-Reynolds-number turbulence. Data analyses are now underway. Here we present some results obtained by the recent data analyses and visualization.

### 1.1. Energy spectrum in the near dissipation range

The energy spectrum in the near dissipation range of turbulence is studied by using the above data set. The spectrum normalized by  $(\langle \epsilon \rangle \nu^5)^{1/4}$  fits well to the form  $C(k\eta)^\alpha \exp(-\beta k\eta)$  in the wavenumber range  $0.5 < k\eta < 1.5$ . The data show that the constants  $\alpha, \beta$  decrease monotonically with  $R_\lambda$  in the simulated  $R_\lambda$  range. The data are also consistent with the conjecture that they approach to constants as  $R_\lambda$  goes to infinity.

1.2. Spectra of dissipation, enstrophy, and pressure

The statistics of the dissipation rate  $\epsilon$  play key roles in many turbulence theories including those by Kolmogorov and Obukhov, while the statistics of the enstrophy  $\Omega = \omega^2/2$  and pressure  $p$  are also the key ingredients of turbulence theories. In incompressible fluid,  $D = \epsilon/(2\nu)$  and  $\Omega$  are related to  $p$  as  $-\Delta p = \rho(D - \Omega)$  and all these quantities are second order in velocity gradients, where  $\rho$  is the fluid density. All of the spectra  $E_D(k)$ ,  $E_\Omega(k)$  and  $E_{\Delta p}(k)$  are written in the form  $E_f(k) = \sum_{|\mathbf{p}|=k} \langle \hat{f}(\mathbf{p}) \hat{f}(-\mathbf{p}) \rangle$ , with  $\hat{f}(k) = C_{abcd} \sum_{\mathbf{k}=\mathbf{p}+\mathbf{q}} P_a Q_b U_c(\mathbf{p}) U_d(\mathbf{q})$ , where  $\sum_{\mathbf{k}=\mathbf{p}+\mathbf{q}}$  denotes the sum over  $\mathbf{p}$  and  $\mathbf{q}$  satisfying  $\mathbf{p}+\mathbf{q}=\mathbf{k}$ , and  $C_{abcd}$  is a fourth order constant tensor. ([3]) Figure 1 shows the spectra  $E_D(k)$  and  $E_\Omega(k)$  obtained by the DNSs in series 1 (up to  $N = 2048$ ). The figure shows that (i) the difference between the spectra for  $f = \epsilon/\nu$  and  $\omega^2$  in each of the four runs is very small over a certain wave number range at small  $k$ , but (ii) the difference is much larger at higher  $k$ , (iii) the greatest difference is at  $k\eta \sim 0.4$ , and (iv) there exists a wave number range (inertial subrange) in which the spectra scale like  $k^{-a}$  with  $a \sim 2/3$ , which is very different from the value obtained by assuming the joint probability distribution of the velocity field

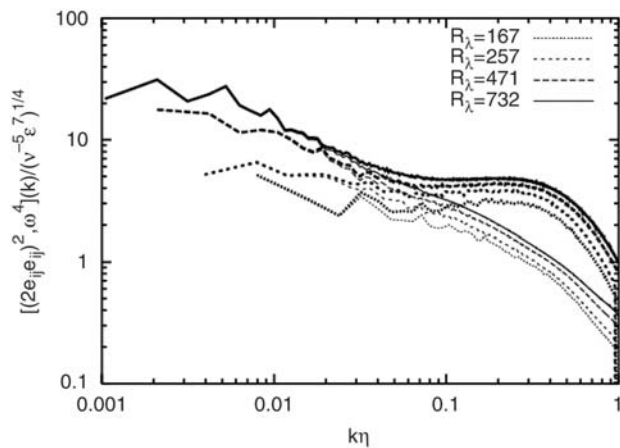


Fig. 1 Spectra  $E_f(k)$  for  $f = \epsilon/\nu$  (thin curves) and  $\omega^2$  (thick curves) (from Ref. [1])

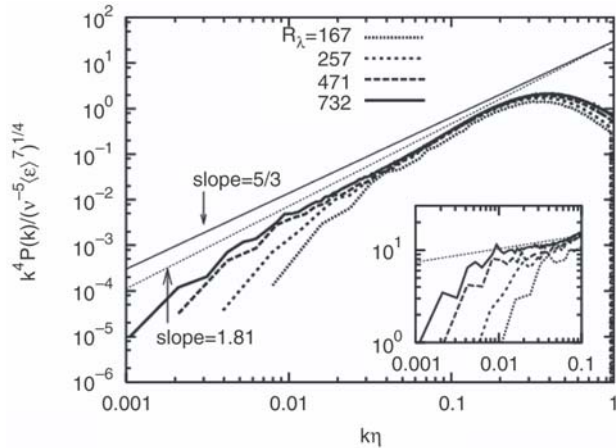


Fig. 2 Spectra  $E_f(k)$  for  $f = \Delta p$ . The inset is the compensated spectra  $E_f(k)/((k\eta)^{5/3} (\nu^5 \langle \epsilon \rangle^7)^{1/4})$  for  $0.001 < k\eta < 0.1$ ; the straight line shows the slope  $k^{1.81-5/3}$ . (from Ref. [1])

to be Gaussian. On the other hand, Figure 2 shows that spectra  $E_{\Delta p}(k)$  behave like  $k^b$  with  $b \sim 5/3$ , which is in good agreement with the Gaussian value. The difference among  $E_D(k)$ ,  $E_\Omega(k)$  and  $E_{\Delta p}(k)$  comes only from the difference in  $C_{abcd}$ . It is therefore unlikely that any theory discarding the tensorial dependence of  $C_{abcd}$  would explain the difference.

1.3. Pressure Fluctuations

Static pressure fluctuation is a fundamental quantity contained in the dynamical equation of fluid motion, but it is the least understood quantity due to the difficulty inherent in measuring this term by conventional equipment. Recently pressure fluctuations in turbulence at high Reynolds number were measured experimentally and its accuracy has been tested using the DNS data. Figure 3 shows that probability density function (PDF) of the pressure fluctuations in turbulence obtained by the DNS is in good agreement with that obtained by the experimental measurement of pressure at a Reynolds

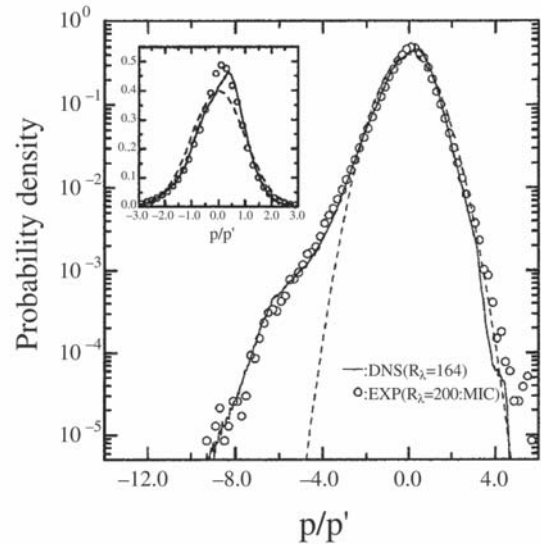


Fig. 3 PDF of measured pressure (symbols) are compared with DNS (solid lines). (from Ref. [2])

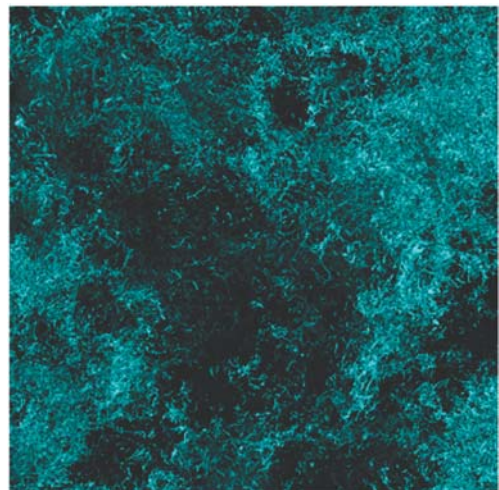


Fig. 4 Intense vorticity regions obtained by the 2048<sup>3</sup> DNS.

number close to the DNS. It was also found that scaling property of the measured pressure spectrum is also consistent with the DNS data.

#### 1.4. Visualization

The data size generated by DNS on advanced computing system such as the ES is generally so huge that it is important to efficiently deal with the data for the understanding of the physics of turbulence. For this purpose, it is helpful to use graphic visualization of the flow field. Figure 4 is an example of such visualization, and shows intense vorticity regions obtained by the 20483 DNS. The visualization of flow fields at high Reynolds number DNSs gives an impression quite different from that at low or moderate Reynolds number DNSs, and suggests the importance of the study of the structure of the cluster of eddies, rather than that of the eddies themselves.

## 2. Simulation of Wind Turbine Tip noise using Large Eddy Simulation

An application for modeling of engineering turbulent flow was also performed as part of this project. The far field broadband noise caused by a rotating wind turbine blade was computed, with particular emphasis on tip noise. The shape of the blade tip has a considerable effect on the overall noise emitted by a wind turbine in operation ([4]). There is a strong need for numerical simulation of aerodynamic tip noise to identify the mechanisms of tip vortex formation and tip noise in order to be able to propose noise reducing design concepts for the outer blade.

#### 2.1. Numerical Methods

It has been recognized that Large Eddy Simulation (LES) is necessary for accurate prediction of aerodynamic noise since conventional CFD methods do not resolve the complete frequency spectrum. However, LES requires a large number of computational grid points to resolve the smallest eddy scales. The prediction of aerodynamic tip noise emitted from a wind turbine blade requires the analysis of vortical structures and pressure fluctuations associated with the tip vortex and their interaction with the trailing edge. Since the compressible Navier-Stokes equations contain the equations governing wave propagation, they are able to model the acoustic field directly and simultaneously in addition to the noise generating flow field. In this work, compressible LES is used to simulate the flow and acoustic field simultaneously in the region near the blade, called the near field. This is called a direct noise simulation. The far field aerodynamic noise caused by the wind turbine blade is predicted by the Ffowcs Williams-Hawkings (FW-H) equation, using the near field results from LES as an input. Simulations are performed for two blade tip geometries, using a very fine grid to resolve the smallest eddy scales.

Figure 5 shows the outline of WINDMELIII as well as the

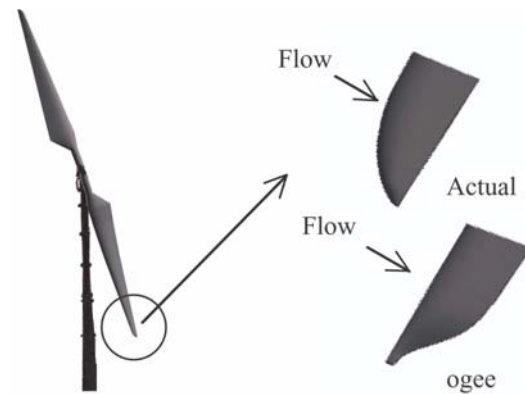


Fig. 5 WINDMELIII

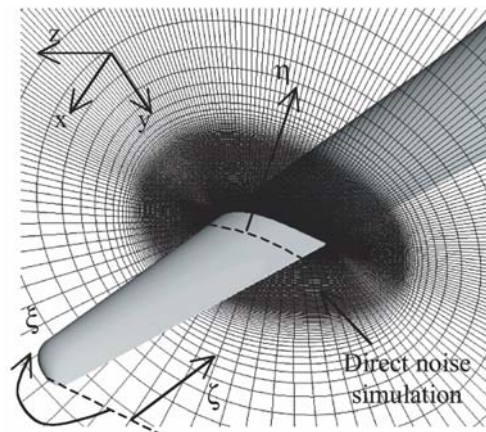


Fig. 6 Computational grid of airfoil section

two blade tip shapes studied. WINDMELIII is a two-bladed wind turbine of upwind type. The Reynolds number at the tip at design condition is approximately 1 million. The actual tip shape of WINDMELIII and a noise reducing ogee type tip shape were simulated. The ogee type tip shape has been shown in field tests to reduce acoustic emissions of wind turbines ([4]). The direct simulation of the acoustic field is performed in the domain with a fine grid lying approximately two chord lengths away from the blade surface, as seen in Fig. 6. The total number of grid points is approximately 300 million. Since the main interest of this research is tip noise, the computational grid in the tip region of the blade is made extremely fine to accurately simulate the tip vortex and to resolve the noise causing high frequency pressure fluctuations inside the tip vortex. The grid spacings in the near blade region are set according to the observations made in the validation part of the present numerical approach ([5]). The simulation was performed on 14 nodes. It takes about 300 CPU hours per processor to simulate a rotation of 10 degrees.

#### 2.2. Results

The vorticity isosurfaces  $\omega_x$  in the tip region can be seen in Fig. 7 for both tip shapes. Very complex three dimensional vortical flow structures associated with the tip vortex can be identified. Vortical structures in the vicinity of a body cause

intense noise. For both tip shapes these vortical structures prevail in the immediate vicinity of the trailing edge, suggesting the importance of the tip vortex-trailing edge interaction as a noise contribution. Concerning the actual tip shape, a major part of the vortical structures can be identified at the immediate tip and in the tip vortex. As for the ogee type tip shape, the tip vortex structure is smoother. Reduced tip vortex shedding and interaction with the trailing edge suggests reduction of noise for the ogee type tip shape. There is, however, some degree of interaction between the vortical structures and the trailing edge further inboard. The change in the blade tip shape does not affect the overall aerodynamic performance of the wind turbine blade.

Figure 8 shows the instantaneous acoustic pressure perturbation field of the wind turbine blade with ogee type tip shape. It can be seen that the noise source lies in the tip region, with acoustic waves propagating away from the tip. The pressure perturbations contain contributions mainly from the fluctuations associated with the tip vortex and its interaction with the trailing edge of the wind turbine blade.

The effect of the blade tip shape on the overall far field noise level at specific observer locations is investigated. The simulated acoustic pressure spectra for the actual and the ogee type tip shapes are shown in Fig. 9 for two far field observer locations, 20 m and 80 m upstream of the wind turbine. The spectra are predicted by simulating the propagation of the pressure fluctuations using LES in the near field and FW-H method in the far field. At a distance of 20 m, the use of an ogee type tip shape can reduce the noise level for frequencies above 4 kHz by up to 5 dB. The reduced acoustic emission of

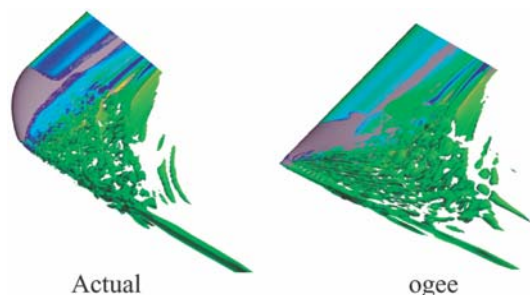


Fig. 7 Vorticity  $\omega_x$  Isosurfaces  
(Color denotes pressure)

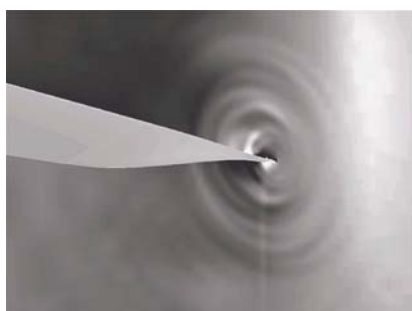


Fig. 8 Instantaneous acoustic pressure perturbation field at blade tip

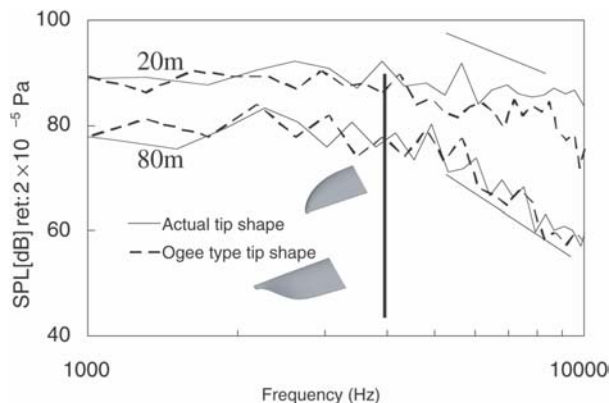


Fig. 9 Sound pressure level at two locations – Simulation results

the ogee type tip shape is likely to be related to the decreased interaction between the tip vortex and the trailing edge. The analysis of the pressure fluctuations in the immediate vicinity of the blade showed that the actual tip shape exhibits very high frequency pressure fluctuations that do not appear for the ogee type tip shape. At a distance of 80 m from the wind turbine, the actual tip shape and the ogee type tip shape do not show any difference in overall sound pressure level. The high frequency contribution decays fairly rapidly in the far field. An overall noise reduction of 14 dB can be observed as compared to the noise level perceived 20 m away from the wind turbine.

By performing more detailed studies of turbulence dynamics and wave propagation in the immediate vicinity of the tip through direct noise simulations, new insights into the physical mechanisms causing tip vortex flow and tip noise can be obtained. The simulation results will contribute towards designing suitable rotor blades with reduced acoustic emission for future large wind turbines operating at higher tip speed ratios.

**References**

- 1) T. Ishihara, Y. Kaneda, M. Yokokawa, K. Itakura, and A. Uno, "Spectra of energy dissipation, enstrophy and pressure by high-resolution direct numerical simulations of turbulence in a periodic box", *J. Phys. Soc. Jpn.* 72, 983–986, 2003.
- 2) Yoshiyuki Tsuji and Takashi Ishihara, "Similarity scaling of pressure fluctuation in turbulence", *Phys. Rev. E*, 68 02630968-1\_5, 2003.
- 3) Y. Kaneda, "High resolution direct numerical simulation of turbulence", to appear in the Proc.of 10th Euromech European Turbulence Conference. 2004.
- 4) S. Wagner, R. Bareis, and G. Guidati, *Wind turbine noise*, Springer-Verlag, Berlin, 1996.
- 5) O. Fleig, C. Arakawa, "Large-Eddy Simulation of Tip Vortex Flow at High Reynolds number", AIAA 2004-0263, 42nd AIAA Aerospace Sciences Meeting and Exhibit, Reno, USA, Jan. 2004.